Conversion of broadband incoherent pump to narrowband signal in an optical parametric amplifier

V. Pyragaite,* V. Smilgevičius, R. Butkus, A. Stabinis, and A. Piskarskas
Department of Quantum Electronics, Vilnius University, Saulėtekio Avenue 9, Building 3, LT-10222 Vilnius, Lithuania
(Received 3 June 2013; published 13 August 2013)

The parametric amplification of the signal beam with a narrow angular spectrum in the field of an incoherent broadband pump is investigated theoretically as well as experimentally. It is demonstrated that in the absence of beam walk-off a significant enhancement of the parametric gain takes place, and the power of the incoherent pump can be effectively transferred into the signal beam. The background of the signal spectrum appearing in the process of amplification due to pump amplitude fluctuations can be removed by filtering, and the coherence of the input signal can be recovered.

DOI: 10.1103/PhysRevA.88.023820 PACS number(s): 42.25.Kb, 42.65.Yj

I. INTRODUCTION

A fundamental question is whether incoherent light can be transferred with high efficiency to coherent light by means of nonlinear optics. To our knowledge, this problem was first discussed in the 1960s. It was pointed out that coherent excitation of a single signal wave is possible for parametric interactions when the signal is coupled to a set of pump waves through a corresponding set of idler waves [1]. In this case the parametric gain is independent of the phases of the pump waves involved, and the pump incoherence is transferred to the idler waves. Afterwards, the driving of a single signal mode by combining the action of mutually incoherent longitudinal modes in a parametric oscillator was experimentally observed in Ref. [2]. Such cumulative action also takes place in parametric systems pumped by several intersecting beams of the same [3] or different [4,5] frequencies. The cumulative action is also typical for parametric processes excited by conical (for example, Bessel) beams [6]. The wave propagating along the pump-cone axis can be phase matched with an infinite set of pump plane waves whose wave vectors are lying on the pump cone. The azimuthal incoherence of the pump beam is transferred to the idler conical beam. A major benefit emerging from the use of a multiple-beam pump is that incoherent, low-power pump sources can be used to amplify a signal beam, thus increasing the output power of optical parametric chirped pulse amplifiers (see Ref. [7] and references therein).

An excitation of a coherent signal wave in the process of down conversion of an incoherent plane pump wave with a continuous spectrum was analyzed in detail in Refs. [8–14]. The excitation is possible if the group velocities of the pump and idler waves are equal (group-velocity matched). The walk-off of the signal wave with respect to the pump and idler waves is a key factor due to which the parametric gain of the signal wave depends only on the average intensity of the pump wave. The incoherence of the pump is absorbed by the idler wave. In this case an exact phase-matching condition is fulfilled only for one (central) frequency component of the signal wave, and the signal wave grows from the quantum noise level with an increasing degree of coherence. As a result, under propagation in the nonlinear medium a signal wave with a high degree of coherence becomes coupled to the incoherent broadband pump through an incoherent broadband idler wave. It is feasible that such coupling could also take place in the optical parametric amplifier (OPA) pumped by broadband incoherent light when a narrowband signal seed is available at the input.

In this paper we demonstrate that the parametric gain of the signal beam in a OPA pumped by an incoherent beam is also effective in the absence of signal walk-off. The correlation functions and angular spectra of the signal and idler beams are obtained. The appearance of the background in the angular spectrum of the amplified signal beam and its removal by the filtering are discussed. A good qualitative agreement with experimental data is obtained. The possibilities to enhance the spectral intensity and to deplete the whole angular spectrum of pump are shown by means of numerical simulations in the nonlinear regime. Therefore the effective conversion of incoherent broadband light to a narrowband signal is possible in the optical parametric amplifier in the absence of beam walk-off.

The rest of this paper is organized as follows. In Sec. II the correlation functions, angular spectra, and intensities of the signal and idler beams are analyzed. The experimental results are presented in Sec. III. An evolution of the signal seed in the parametric amplifier in the case of pump depletion is discussed in Sec. IV. Conclusions are presented in Sec. V.

II. THEORETICAL ANALYSIS

We consider the propagation of three monochromatic interacting beams in a quadratic nonlinear medium along z neglecting walk-off as well as diffraction. In this case the amplitudes A_j, $j = 1,2,3$, of three waves obey the coupled differential equations:

$$\frac{\partial A_1}{\partial z} = \sigma_1 A_2^* A_3, \tag{1a}$$

$$\frac{\partial A_2}{\partial z} = \sigma_2 A_1^* A_3, \tag{1b}$$

$$\frac{\partial A_3}{\partial z} = -\sigma_3 A_1 A_2, \tag{1c}$$

where $\sigma_j = d_{\mathrm{ef}} k_j / n_j^2$ stands for the nonlinear coupling coefficient of the jth wave, whose frequency is ω_j. d_{ef} is the effective second-order susceptibility, $k_j = \omega_j n_j / c$ is a wave number, and n_j is a refractive index. For definiteness we call

*viktorija.pyragaite@ff.vu.lt

 ©2013 American Physical Society

the first, second, and third waves the signal, idler, and pump beams, respectively.

We assume that at the input of OPA the pump and signal beams are homogeneous and uncorrelated and obey Gaussian statistics as well as the Gaussian autocorrelation function. For simplicity we restrict our analysis to the two-dimensional case (x,z). We can write

$$B_{j0}(d) = \langle A_{j0}(x+d)A_{j0}^{*}(x)\rangle = \langle a_{j0}^{2}\rangle \exp\left(-\frac{d^{2}}{\rho_{j}^{2}}\right), \quad (2)$$

$j = 1,3$. Here x is a transverse coordinate, and $B_{j0}(d)$ and $A_{j0}(x)$ are the correlation function and amplitude at the input of the nonlinear crystal, respectively. $\langle a_{j0}^{2}\rangle = \langle |A_{j0}|^{2}\rangle$ stands for the normalized mean intensity, and ρ_j is the correlation radius of the jth beam. Here we neglect pump depletion and assume no idler beam at the input, $A_{20}(x) = 0$. Then the solutions of Eqs. (1) read

$$A_{1}(z,x) = A_{10}\cosh[\sqrt{\sigma_{1}\sigma_{2}}|A_{30}(x)|z], \quad (3a)$$

$$A_{2}(z,x) = \sqrt{\frac{\sigma_{2}}{\sigma_{1}}}A_{10}^{*}(x) \times \exp[i\varphi_{30}(x)]\sinh[\sqrt{\sigma_{1}\sigma_{2}}|A_{30}(x)|z], \quad (3b)$$

where $\varphi_{30}(x)$ is a pump phase. Obviously, the parametric gain of the signal wave is independent of pump phase fluctuations [see Eq. (3a)]. The correlation functions of the output signal and idler beams $B_1(d)$ and $B_2(d)$ are found from

$$B_{1}(d) = B_{10}(d)\langle\cosh(pb)\cosh(p_{d}b)\rangle, \quad (4a)$$

$$B_{2}(d) = \frac{\sigma_{2}}{\sigma_{1}}B_{10}(d)\langle\exp[i(\phi_{d}-\phi)] \times \sinh(pb)\sinh(p_{d}b)\rangle, \quad (4b)$$

where $p(x) = |A_{30}(x)|/\sqrt{\langle a_{30}^{2}\rangle}$, $b = z/L_n$, $L_n = 1/\sqrt{\sigma_1\sigma_2\langle a_{30}^{2}\rangle}$ is a nonlinear interaction length, $p_d = p(x+d)$, $\phi = \varphi_{30}(x)$, and $\phi_d = \varphi_{30}(x+d)$.

In the case of the homogeneous Gaussian stochastic process with complex amplitude $A = \frac{a(x)}{2}\exp[i\phi(x)] = [\xi_1(x) + i\xi_2(x)]/2$, where $\xi_1 = a\cos(\phi)$, $\xi_2 = a\sin\phi$, and $\langle\xi_1\rangle = \langle\xi_2\rangle = 0$, $\langle\xi_1\xi_2\rangle = 0$, an envelope $a(x)$ obeys the Rayleigh distribution, the phase $\phi(x)$ is uniformly distributed in the interval $[0,2\pi]$, and the quantities ξ_1, ξ_2 obey Gaussian distribution [15]. The average values in Eqs. (4) can be found if the distribution $w(p,p_d,\phi,\phi_d)$ is available. This distribution can be obtained by the transformation of the four-dimensional Gaussian distribution $w(\xi_1,\xi_2,\xi_{1d},\xi_{2d})$. As a result, we have

$$w(p,p_{d},\phi-\phi_{d}) = \frac{pp_{d}}{16\pi^{2}(1-R^{2})} \times \exp\left(-\frac{p^{2}+p_{d}^{2}-2pp_{d}R\cos(\phi-\phi_{d})}{4(1-R^{2})}\right), \quad (5)$$

where $R(d) = B_{30}(d)/\langle a_{30}^{2}\rangle$ is a normalized correlation function of the pump beam. Using Eqs. (4) and (5) and integrating over phases ϕ and ϕ_d, the correlation functions B_1 and B_2 can be expressed as double integrals:

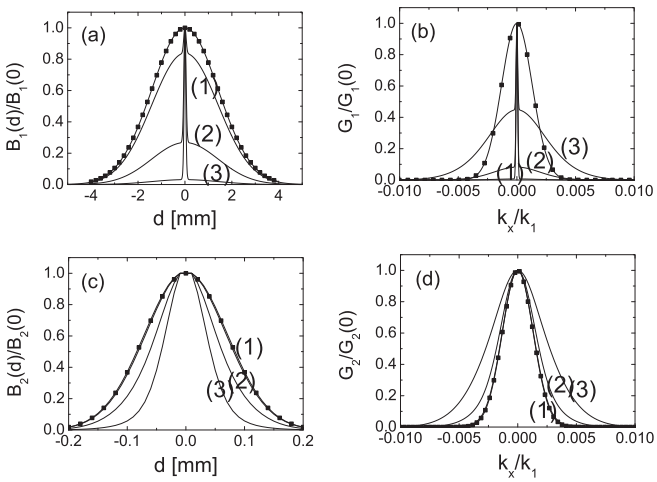

FIG. 1. (a) and (c) Correlation functions and (b) and (d) angular spectra of (a) and (b) the output signal and (c) and (d) idler beams. The squares correspond to the input signal beam in (a) and pump beam in (b)–(d). z/L_n is 0.5, 1, and 1.5 for curves 1, 2, and 3, respectively. $\rho_1 = 2$ mm, $\rho_3 = 100$ μm.

$$B_{1}(d) = B_{10}(d)\int_{0}^{\infty}\int_{0}^{\infty}\cosh(pb)\cosh(p_{d}b) \times w_{0}(p,p_{d})dpdp_{d}, \quad (6a)$$

$$B_{2}(d) = \frac{\sigma_{2}}{\sigma_{1}}B_{10}(d)\int_{0}^{\infty}\int_{0}^{\infty}\sinh(pb)\sinh(p_{d}b) \times w_{1}(p,p_{d})dpdp_{d}, \quad (6b)$$

where

$$w_{0,1}(p,p_{d}) = \frac{pp_{d}}{4(1-R^{2})}I_{0,1}\left(\frac{R}{2(1-R^{2})}pp_{d}\right) \times \exp\left(-\frac{p^{2}+p_{d}^{2}}{4(1-R^{2})}\right) \quad (7)$$

and $I_{0,1}$ is a modified Bessel function.

The integrals (6) were calculated numerically. The Fourier transform was applied, and the angular spectrum $G_j(k_x)$ of the output beams was obtained. The results are presented in Fig. 1. The degenerate regime was assumed, $\sigma_1 = \sigma_2$. The wave number k_1 corresponds to the signal beam in type-II KTP (Potassium titanyl phosphate) crystal for signal wavelength $\lambda_1 = 1.064$ μm.

The correlation function of the signal beam at $\rho_1 \gg \rho_3$ is composed of the sharp, narrow central part (spike) and the background [Fig. 2(a)]. The spike appears due to pump amplitude fluctuations and determines the background of the signal spectrum. On the other hand, the spike in the spectrum appears due to the background of the correlation function. We note that the shapes of the correlation function and the spectrum of the idler beam [Figs. 1(c) and 1(d)] do not depend on the correlation radius ρ_1 if $\rho_1 \gg \rho_3$. Using the Rayleigh distribution $w(p) = \frac{p}{2}\exp(-p^2/4)$, the intensities $B_1(0)$ and $B_2(0)$ of the signal and idler beams, respectively, can be found

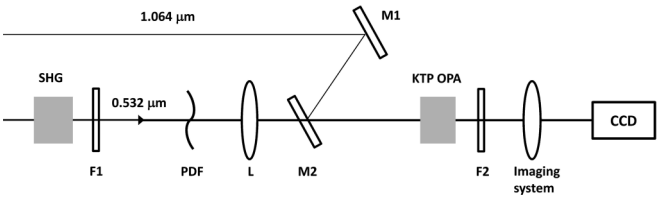

FIG. 2. Experimental setup.

analytically:

$$B_1(0) = B_{10}(0)[1 + \sqrt{\pi} b \exp(4b^2)\mathrm{erf}(2b)], \quad (8a)$$

$$B_2(0) = B_1(0) - B_{10}(0), \quad (8b)$$

where $\mathrm{erf}(t) = \frac{2}{\sqrt{\pi}} \int_0^t \exp(-t'^2) dt'$. At $b \geqslant 1$ Eq. (8a) can be written as

$$B_1(0) \approx \sqrt{\pi} B_{10}(0) b \exp(4b^2). \quad (9)$$

We note that due to pump amplitude fluctuations the parametric gain of the signal intensity is significantly enhanced compared to a gain in the field of a coherent plane pump wave of the same intensity, where $B_1(0) \sim \exp(2b)$ at $b \gg 1$. An intensity $B_{1b}(0)$ of the signal-beam background can be evaluated as

$$B_{1b}(0) \approx B_{10}(0)\langle \cosh(pb)\rangle^2 = B_{10}(0)[1 + \sqrt{\pi} b \exp(b^2)\mathrm{erf}(b)]^2, \quad (10)$$

and the ratio $\eta = B_1(0)/B_{1b}(0)$ of the spike and the background intensities is

$$\eta = \frac{1 + \sqrt{\pi} b \exp(4b^2)\mathrm{erf}(2b)}{[1 + \sqrt{\pi} b \exp(b^2)\mathrm{erf}(b)]^2}. \quad (11)$$

For $b = z/L_n = 0.5, 1, 1.5$ we obtain $\eta = 1.2, 3.8, 33.5$, respectively [see Fig. 1(a)]. The background of the signal spectrum is more significant when the crystal length $b = z/L_n$ is larger and is less significant for larger values of the correlation radius ρ_1. The background of the signal angular spectrum can be removed by filtering, and as a result, the coherence of the input signal beam can be recovered.

III. EXPERIMENTAL RESULTS

The experimental setup of a degenerate OPA is presented in Fig. 2. We used a picosecond laser system which consisted of an oscillator, a Nd:YAG low-gain regenerative preamplifier, and two parallel amplifiers APL2210B (UAB Ekspla) which served as a source for pump and seed beams. The system generated $\tau = 50$ ps pulses at a repetition rate of 1 kHz. The fundamental harmonic from one channel was attenuated and was used as a seed for the OPA. Its angular spectrum is depicted in Figs. 3(a) and 3(b). The signal Gaussian beam radius was about ∼0.6 mm, and input energy was ∼95 nJ. The fundamental harmonic pulses from the second channel were passed through a 3-cm-long type-II KDP (Potassium dihydrogen phosphate) frequency-doubling crystal and produced ∼0.3 mJ of second-harmonic (SH; 532 nm) radiation, which was used to pump degenerate KTP OPA (1-cm-long, type-II phase matching, $\varphi = 23.5^\circ$, $\theta = 90^\circ$). The SH beam radius was ∼1 mm. Filter F1 was used to block completely the fundamental harmonic beam and pass the SH radiation. The phase distortion film (PDF) was placed behind SH crystal to

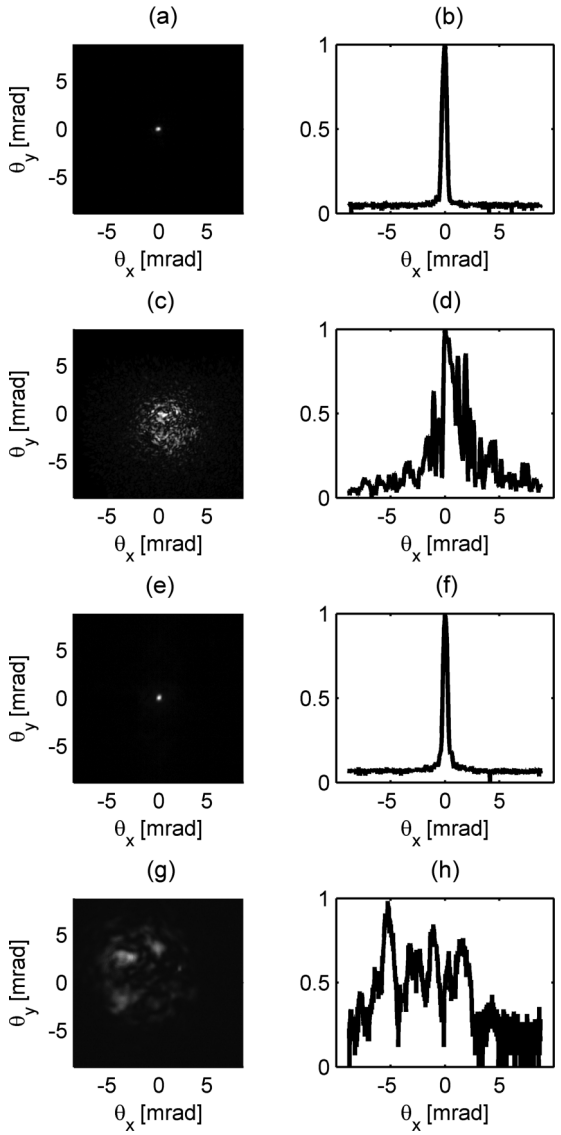

FIG. 3. Experimental angular spectra of (a) and (b) the input signal, (c) and (d) input pump, (e) and (f) output signal, and (g) and (h) output idler beams. The signal energy is amplified by a factor of ∼3.5. The square root of the intensity is depicted.

form spatially incoherent radiation for OPA pump. The Fourier spectrum of the OPA pump radiation is presented in Figs. 3(c) and 3(d). The incoherent OPA pump beam was focused by a 50-cm focal length lens. Both pump and seed radiations were spatially and temporally overlapped in KTP crystal.

For the case of rather low parametric gain (pump energy of 185 μJ) the output signal and idler angular spectra are depicted in Figs. 3(e)–3(h). The background of the output signal spectrum is negligible [compare Figs. 3(f) and 1(b), curve 1]. The width of the angular spectrum of the pump beam was evaluated as $\Delta\theta \approx 5$ mrad [Fig. 3(d)], which corresponds to an experimental correlation radius $\rho_3^{\mathrm{exp}} \approx 65$ μm. With an increase of parametric gain (pump energy of 240 μJ) the background of the output signal spectrum becomes more distinct [compare Fig. 4(b) to Fig. 3(f)]. As can be seen from Figs. 3(g) and 3(h), the idler wave obeys a broad

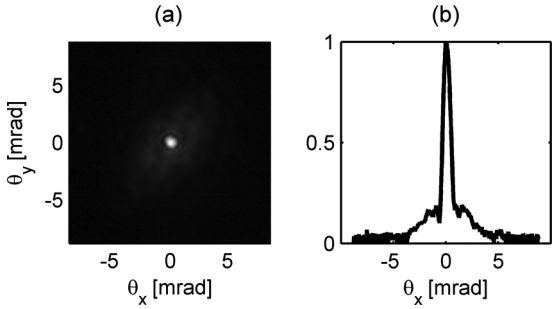

FIG. 4. Experimental angular spectrum of the output signal beam. The signal energy is amplified by a factor of ∼6. The square root of the intensity is depicted.

angular spectrum. The obtained results are in good qualitative agreement with the theoretical predictions.

The governing Eqs. (1) are valid when the walk-off and diffraction of the beams are negligible. In experiment, the type-II KTP crystal was used. The refractive indices and related quantities were taken from [16]. The walk-off angles of the pump and idler beams are 4.1 and 3.2 mrad, respectively. In a 1-cm-long crystal the corresponding walk-off lengths are 41 and 32 μm. These values are smaller than ρ_3^{exp}, so the assumption was correct. On the other hand, the diffraction length $L_{\text{diff}} = k_3(\rho_3^{\text{exp}})^2/2 \approx 4.5$ cm is rather long compared to the crystal length, so the influence of diffraction can also be neglected.

The influence of temporal walk-off can also be neglected. The effective walk-off lengths were calculated from $L_{v,j} = \tau/(|1/u_j - 1/u_3|)$, where $j = 1,2$ and u is a group velocity. We obtain $L_{v,1} = 12$ cm and $L_{v,2} = 43$ cm. As we can see, these lengths are an order larger than the crystal length (1 cm).

IV. NUMERICAL SIMULATION

The results presented above correspond to a linear regime of amplification. The question of how the pump depletion affects the process might arise. Here we perform numerical simulations of the full equations where both diffraction and walk-off terms are included:

$$\frac{\partial A_1}{\partial z} + \frac{i}{2k_1}\frac{\partial^2 A_1}{\partial x^2} = \sigma_1 A_2^* A_3, \tag{12a}$$

$$\frac{\partial A_2}{\partial z} + \beta_2\frac{\partial A_2}{\partial x} + \frac{i}{2k_2}\frac{\partial^2 A_2}{\partial x^2} = \sigma_2 A_1^* A_3, \tag{12b}$$

$$\frac{\partial A_3}{\partial z} + \beta_3\frac{\partial A_3}{\partial x} + \frac{i}{2k_3}\frac{\partial^2 A_3}{\partial x^2} = -\sigma_3 A_1 A_2. \tag{12c}$$

β_j is a walk-off angle. In order to mimic the experimental situation the Gaussian Schell model of the pump beam [17] was used. Then, the amplitude of the pump beam can be written as

$$A_{30}(x) = \sqrt{\langle a_{30}^2\rangle}\exp\left(-x^2/r_3^2\right)\sum_{s=1}^{N_s}\exp(iK_s x + i\gamma_s), \tag{13}$$

where r_3 is the beam-envelope radius, K_s is the random number of normal distribution with variance $\Delta K_3/\sqrt{2}$, where $\Delta K_3 = 2/\rho_3$, and γ_s is a uniformly distributed phase. N_s has to be sufficiently large. The input signal beam was assumed to be a regular Gaussian beam of radius r_1. Equations (12) were simulated N times for a 1-cm-long KTP crystal, and the average values were fixed.

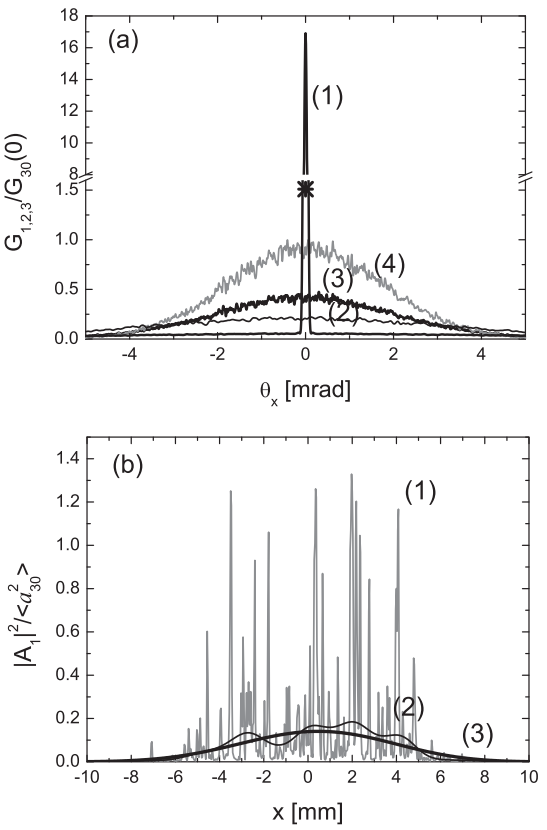

FIG. 5. Numerical simulation of Eqs. (12). (a) Angular spectra of the (1) output signal, (2) idler, and (3) pump beams and (4) the angular spectrum of the input pump beam. The star shows the spectral intensity of the input signal beam. (b) Intensity profile of the amplified signal beam, (1) without filtering and (2) and (3) with filtering applied. The filter bandwidth is $10/r_1$ for curve 2 and $2/r_1$ for curve 3. $L_n = 4$ mm, $r_3 = 8$ mm, $\rho_3 = 68$ μm, $r_1 = 8$ mm, $|A_{10}|/\sqrt{\langle a_{30}^2\rangle} = 0.1$. An average of $N = 500$ simulations is shown in (a) and $N = 1$ simulation in (b).

Figure 5 represents the nonlinear regime of amplification. As we can see, the whole spectrum of the pump beam is depleted [compare curves 3 and 4 in Fig. 5(a)], so the power of the broadband pump is transferred to the narrowband signal beam, which means that the signal beam is coupled to the incoherent pump through an incoherent idler beam. We note that signal angular spectrum obeys a wide background which yields a speckle structure in the intensity profile of a single shot, curve 1 in Fig. 5(b). However, it is possible to make the profile regular by spatial filtering. The filtering was applied in one realization of the numerical simulation. The inverse Fourier transform of the spectrum yields the regular intensity profile, curve 3 in Fig. 5(b), and the coherence of the signal beam is recovered. We note that the results are the same as in the case of simplified Eqs. (1).

If the width of the angular spectrum of the signal beam is rather small, then a significant enhancement of its spectral intensity becomes possible [Fig. 5(a), curve 1]. To demonstrate that, a large radius (8 mm) of the signal beam was used in the simulation.

V. CONCLUSIONS

In conclusion, the parametric amplification of the input narrowband signal in the field of an incoherent broadband pump was analyzed. It was shown that when the walk-off and diffraction of the beams can be neglected, the angular spectrum of the amplified signal is composed of a spike and the background and is free of pump phase fluctuations. The spike is determined by the input signal spectrum, and the background appears due to pump amplitude fluctuations. The background of the signal spectrum can be removed by filtering, and the coherence of the input signal can be recovered. The parametric gain of the signal intensity due to pump amplitude fluctuations is significantly enhanced compared to the gain in the field of a coherent plane pump wave of the same intensity. The obtained experimental results are in good qualitative agreement with the theoretical consideration. By means of numerical simulations we show that in the nonlinear regime the whole pump spectrum is depleted and the spectral intensity of the signal beam becomes larger than that of the pump beam.

The presented results can be directly applied to a time domain when the group-velocity mismatch and group-velocity dispersion of interacting waves can be neglected.

ACKNOWLEDGMENT

This work was supported by the Research Council of Lithuania, Project No. MIP-073/2013.

[1] S. E. Harris, IEEE J. Quantum Electron. **2**, 701 (1966).
[2] R. L. Byer, M. K. Oshman, J. E. Young, and S. E. Harris, Appl. Phys. Lett. **13**, 109 (1968).
[3] V. Smilgevičius and A. Stabinis, Opt. Commun. **106**, 69 (1994).
[4] A. Marcinkevičius, A. Piskarskas, V. Smilgevičius, and A. Stabinis, Opt. Commun. **158**, 101 (1998).
[5] G. Tamošauskas, A. Dubietis, G. Valiulis, and A. Piskarskas, Appl. Phys. B **91**, 305 (2008).
[6] A. Piskarskas, V. Smilgevičius, and A. Stabinis, Opt. Commun. **143**, 72 (1997).
[7] A. Piskarskas, A. Stabinis, and V. Pyragaite, IEEE J. Quantum Electron. **46**, 1031 (2010).
[8] A. Picozzi and M. Haelterman, Phys. Rev. E **63**, 056611 (2001).
[9] A. Picozzi, C. Montes, and M. Haelterman, Phys. Rev. E **66**, 056605 (2002).
[10] A. Picozzi and M. Haelterman, Phys. Rev. Lett. **92**, 103901 (2004).
[11] A. Picozzi and P. Aschieri, Phys. Rev. E **72**, 046606 (2005).
[12] S. Wabnitz, A. Picozzi, A. Tonello, D. Modotto, and G. Millot, J. Opt. Soc. Am. B **29**, 3128 (2012).
[13] C. Sun, S. Jia, C. Barsi, S. Rica, A. Picozzi, and J. W. Fleischer, Nat. Phys. **8**, 469 (2012).
[14] V. Pyragaite, A. Stabinis, A. Piskarskas, and V. Smilgevičius, Phys. Rev. A **87**, 063809 (2013).
[15] L. Mandel and E. Wolf, *Optical Coherence and Quantum Optics* (Cambridge University Press, Cambridge, 1995).
[16] A. V. Smith, SNLO nonlinear optics code, AS-Photonics, Albuquerque, NM, 2012.
[17] G. Gbur, Opt. Express **14**, 7567 (2006).